The Monte Carlo Method: Versatility Unbounded in a Dynamic Computing World
Chattanooga, Tennessee, April 17-21, 2005, on CD-ROM, American Nuclear Society, LaGrange Park, IL (2005)

THE LIÈGE INTRANUCLEAR CASCADE MODEL. PRESENT STATUS.

Th. Aoust
SCK·CEN
Reactor Physics and MYRRHA Department
Boeretang 200, B-2400 Mol, Belgium
taoust@sckcen.be

J. Cugnon and P. Henrotte
Physics Department
University of Liège
Allée du 5 Août 17, Bât. B5, B-4000, Liège 1, Belgium

A. Boudard, J.C. David, S. Leray and C. Volant
DAPNIA SPhN
CEA Saclay
F-91191 Gif-sur-Yvette Cedex, France

ABSTRACT

Spallation reactions are usually simulated by intranuclear cascade model followed by evaporation-fission models. In the intranuclear cascade step, the particle-nucleus collision is described by Monte Carlo simulations of the nucleon-nucleon collisions inside the nucleus. Tested against many experimental measurements, the intranuclear cascade of Liège (INCL) has been shown to be quite successful in the description of proton-induced spallation reactions in the 200 MeV - 2 GeV range. In this paper, the capabilities of INCL4 and the more recent improvements of the model are presented. They bear on the introduction of an isospin and energy dependence of the mean field, on the improvement of the pion production mechanism, on the behaviour of the model at low energy and on the inclusion of composite production during the cascade stage.

Key Words: Spallation reaction, nuclear data

1 INTRODUCTION

Nucleon-nucleus reactions from some hundreds of MeV to some GeV energy range are called spallation reactions. Spallation reactions occur in the space and in the vicinity of intermediate energy accelerators. Spallation reactions are important in medicine, in cosmic ray physics and in astrophysics. Recently the interest of spallation reactions induced by proton has been renewed with the development of accelerator driven system (ADS) for the transmutation of nuclear waste [1]. Therefore the use of reliable spallation reaction models embedded into transport codes are of primary importance. In view of the physics of the spallation, the easiest way to simulate these reactions is to use Monte Carlo algorithms based on the basic features of

nuclear dynamics in the collision regime. The number of particles to track and the number of open channels make quasi impossible the use of deterministic approaches. Nevertheless , recent theoretical progresses indicate that the INC Monte Carlo technique (with a mean field) is equivalent to solve a microscopically derived (intranuclear) transport equation [2, 3] for the average one body distribution functions. However, the INCL model can handle all kinds of particle-particle correlations contained in higher-order distributions functions [4].

The spallation reaction is currently described by a first brief time stage of intranuclear cascade process governed by nucleon-nucleon collisions, leading to an excited nucleus after ejection of a few energetic particles. Afterward the residual excited nucleus evaporates or fissions during a longer time stage. INCL is the model of intranuclear cascade developped at the university of Liège. In this paper, we will present results of INCL coupled to the ABLA evaporation-fission model developed at GSI [5]. Both these models are now integrated in the Monte Carlo transport code MCNPX [6].

Tested against many experimental measurements, the Liège INC model has been shown to be quite successful in the description of proton-induced spallation reactions in the 200 MeV - 2 GeV energy range. In this paper we will shortly describe the INCL4 model, its capabilities and present recent improvements.

2 THE INCL4 MODEL

The INCL4 version is decribed in detail in ref. [7]. In the beginning of each run, the position and momentum of all target nucleons are randomly distributed in the nuclear volume and in a Fermi sphere, respectively. The incident particle, randomly positionned on the surface, enters the nucleus and makes a cascade of collisions. The choice of the next event (collision, decay or escape) is based on minimum time, and this event is of course subjected to Monte Carlo runs. $NN \rightleftharpoons NN$, $NN \rightleftharpoons N\Delta$ and $\Delta \rightleftharpoons \pi N$ collisions are based on realistic parametrized cross sections and are subjected to Pauli blocking. The cascade is stopped according to a criterion based on the time evolution of some physical quantities afterwards the evaporation code, fed by the cascade, is started.

Typical features of INCL4 are mainly the introduction of a smooth nuclear surface in concordance with electron scattering data and the implementation of a consistent Pauli blocking: collisions are allowed if they passed the test for the Pauli blockers but also if the original Fermi sphere is excited. This lead to a parameter-free code with its own asbsolute normalization (the computed total reaction cross section is correctly reproduced). Neutron and proton energy spectra are well reproduced for a vast set of target nuclei and incident energy [7]. Figs. 1 and 2 compare some spectra obtained with experimental data. Concerning the production of residues, close to the target mass where the cascade dominantly influences the final result, cross sections are correctly reproduced (see Fig. **??**). The fission products are also well predicted by the evaporation/fission code ABLA. Residue production cross sections are systematically underestimated around A=140.

3 IMPROVEMENTS FOLLOWING INCL4

3.1 Isospin and energy dependences of the mean field

In the INCL model, the nucleons are supposed to experience a nuclear mean field, that is represented by a potential well of fixed depth, which is the same for protons and neutrons. Also, the Fermi momentum is taken the same for both species. As a consequence, they have the same separation energy.

This representation of the nuclear mean field is not consistent with the well-established

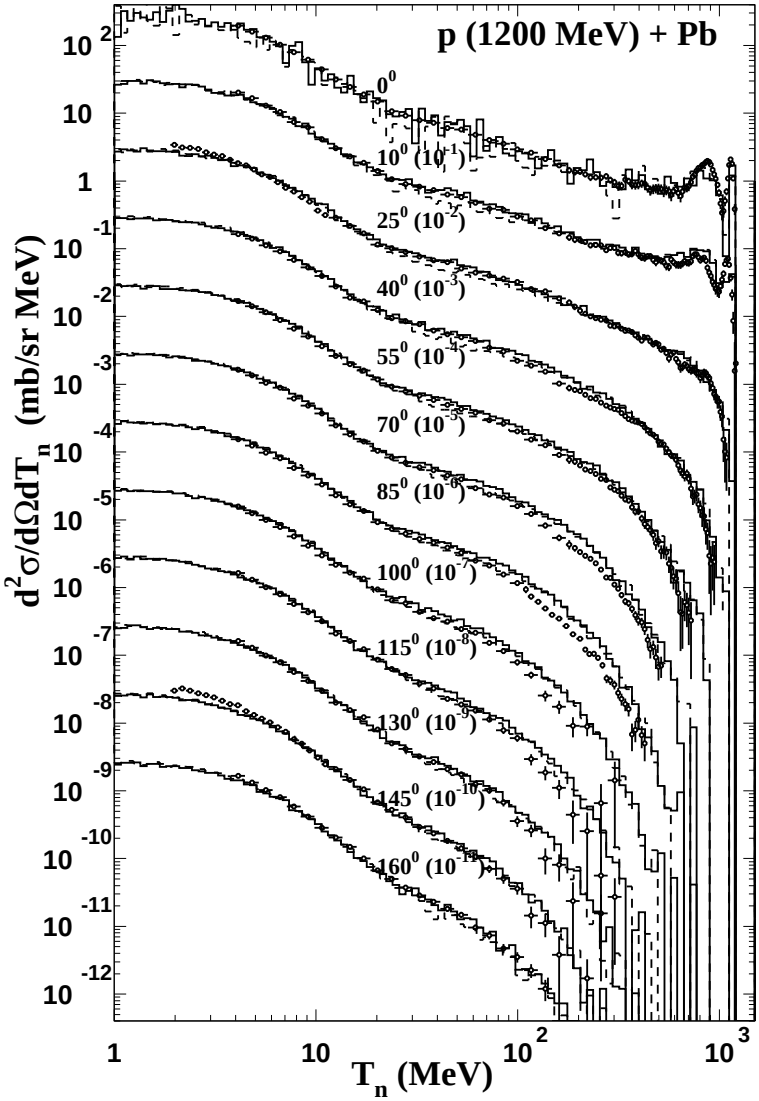

Figure 1: Neutron double differential cross section induced by p(1200 MeV) on ^{208}Pb. Data from [17] are points, results of INCL4+ABLA are histograms with (dashed) and without (continuous) emission of composites. Adapted from [8].

phenomenology of the optical-model potential [14], which is also supported by theoretical arguments [15]. The real part of the potential depends upon the isospin of the nucleons (T_3) and upon their energy (E). Roughly speaking, the depth of the potential is linearly decreasing with the nucleon energy untill the latter reaches $E_0 \sim 200MeV$, beyond which it basically vanishes. The depths of the nucleon potentials (both isospin- and energy-dependent) introduced in INCL (see ref. [16] for more details) are given by

$$V_0^i(E) = V_0^i - \alpha_i(E - E_F^i), \tag{1}$$

where E is the total energy

$$E = \frac{\hbar^2 k^2}{2M} + V_0^i(E), \tag{2}$$

and E_F^i is the Fermi energy

$$E_F^i = \frac{\hbar^2 k_F^{i^2}}{2M} + V_0^i. \tag{3}$$

According to ref. [14], we choose $\alpha_n = \alpha_p = 0.23$.

The effect of introducing these phenomenological potentials are shown in Table I and Fig. 5. The introduction of isospin-dependent nuclear potentials lowers the average multiplicity of neutrons emitted during the cascade stage and slightly increases the corresponding proton multiplicity. This results from the fact that target neutrons (protons) are now sitting, on the average, at lower (higher) energy compared to the Fermi energy. As a secondary effect, the excitation energy has slightly increased, leading to more neutrons during the evaporation stage.

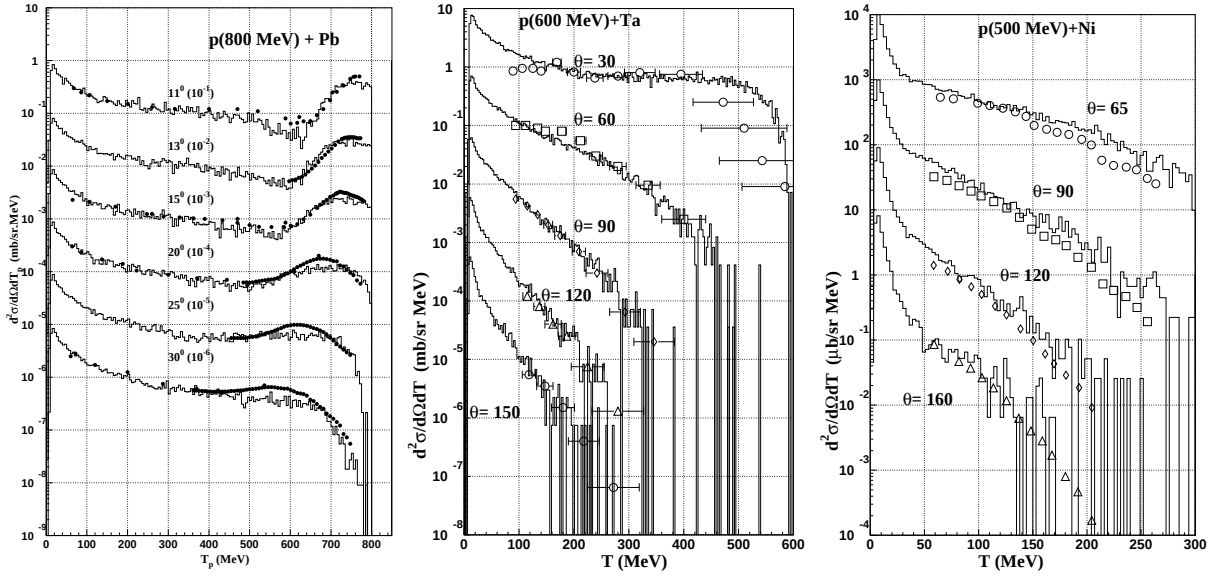

Figure 2: Proton double differential cross section induced by p of 800 MeV on Pb (data points are from [9]), of 600 MeV on Ta (data points are from [10]) and of 500 MeV on Ni (data points are from [11]). The results of INCL4+ABLA are histograms. Adapted from [8].

The further introduction of the energy dependence slightly increase the trends. The shape of the particle spectra are not changed very much, except in the vicinity of the quasi-elastic peak. There is a systematic shift of the quasi-elastic peak towards lower energies.

We also investigated the effect of the average potential for pions (in the standard INCL code $V_0^{\pi} = 0$). In the range of application of intranuclear cascade, produced pions have low and intermediate energies. In this energy range, pion-nucleon reactions are dominated by resonant absorption and the potentials usually used, are functions of the densities of the neutrons and protons (and their derivatives), of the energy, etc. These potentials contain many free parameters which are optimized to fit scattering data. These potentials show us that in the nuclear volume the real potential is largely repulsive and may vary rapidly with energy and in the nuclear surface the

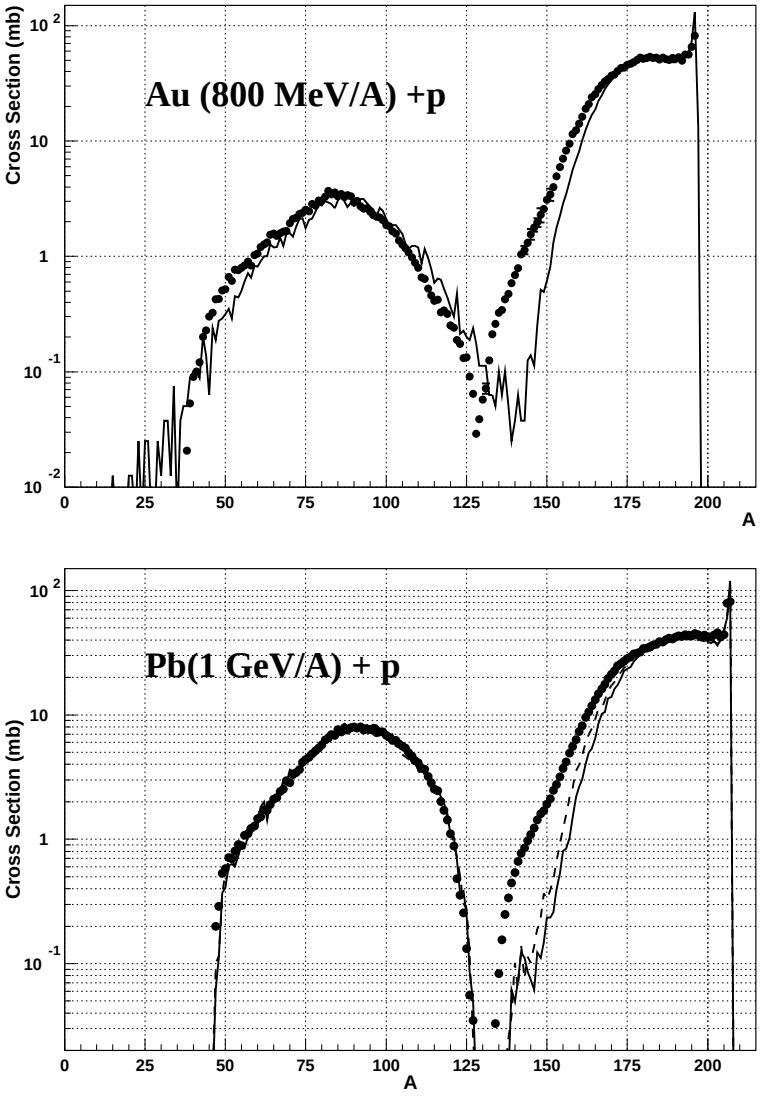

Figure 3: Spallation residues production Cross section induced by p of 800 MeV on Pb and of 1 Gev on Au. Data points are from [12] and [13]. Adapted from [8].

potential is slightly attractive [20]. For a simple investigation of the global effect of pion potential, we introduced an isospin-dependent and energy-independent square-well potential for the pions in the INCL code.

Fig. 6 and 7 display, for various depths of the pion potential, the ratio between calculated yields of positive and negative pions, respectively, and the experimental yield induced by 730 MeV protons on lead. This assessment shows that the use of attractive potentials of $\sim$ 25 MeV leads to the best results. This improves significantly the production of pions (with the original INCL4, C/E = 1.75 for π^+ and 1.67 for π^-). The main contribution to this improvement is the fact that a pion can escape if it reaches the surface and if it can cross over the potential barrier. In the standard INCL4, at the end of the cascade all pions were assumed to have left the nucleus.

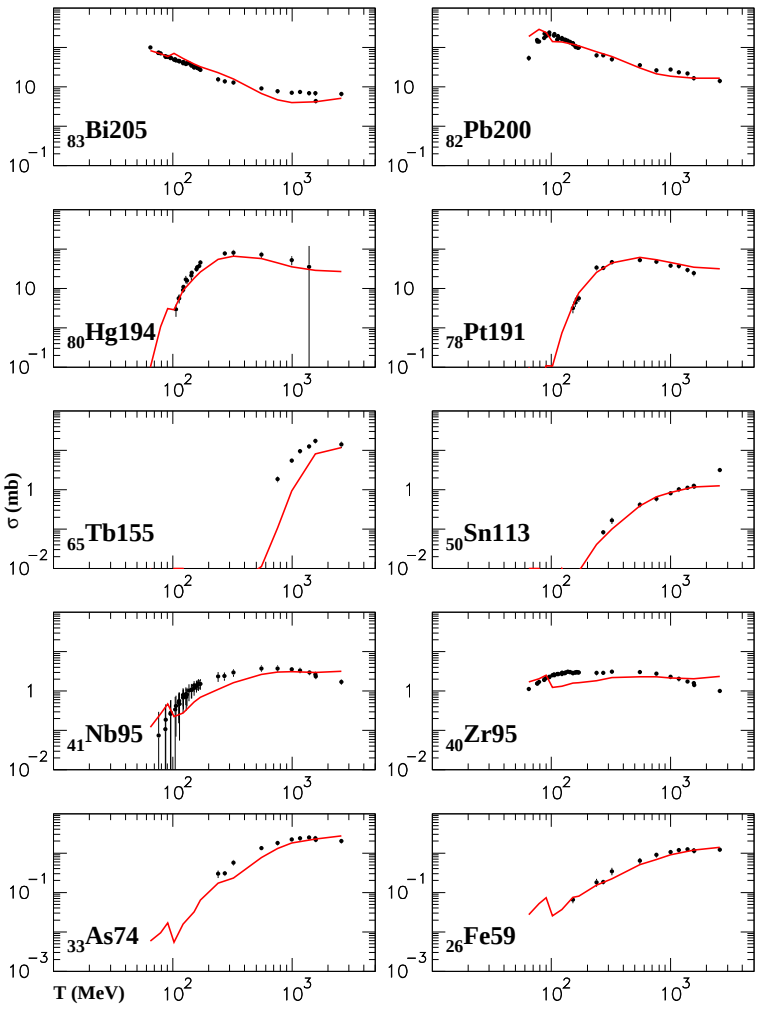

Figure 4: Spallation residues production Cross section induced by p with various energy on Pb. Data are points.

3.2 Low-energy behaviour

The theoretical limit of validity of the intranuclear cascade process is determined by requiring that the successive nucleon-nucleon collisions are well separated in space and time. This independent collision picture is fulfilled when the de Broglie wavelength of the incident nucleon is smaller than the average distance between neighboring nucleons. This condition requires incident energy larger than 100 MeV. One has to keep in mind that, even at high incident energy, the separability of secondary collisions is far from being guaranted. Generally, below 100 MeV incident energy, pre-equilibrium models are used. In the work of ref. [22], the relevance of the INCL model at low incident energy has been examined by comparing its predictions (here

Table I: Multiplicities per primary reaction given by p(800 MeV) + ^{208}Pb. Experimental data are from ref. [17]. Adapted from ref. [18].

	Standard	$V^N(T_3)$	$V^N(T_3, E)$	Exp
n,E $>$ 20 MeV	2.48	2.28	2.21	1.9 ± 0.2
n,E $>$ 2 MeV	9.30	9.26	9.23	10.4 ± 1.4
p,E $>$ 20 MeV	2.07	2.20	2.18	
p,E $>$ 2 MeV	2.55	2.70	2.65	

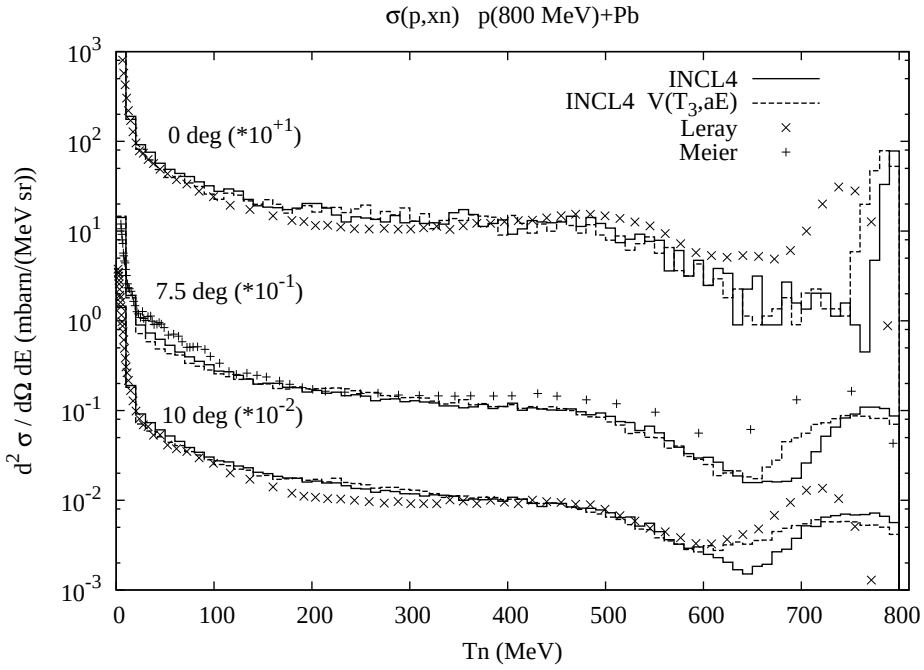

Figure 5: Double differential neutron cross section for 800 MeV proton on ^{208}Pb. Results of INCL4 without (full histograms) and with (dashed histograms) isospin- and energy-dependent potential. Data are taken from refs. [17, 19] .

INCL3) and the available experimental data for proton and neutron double differential cross sections. This investigation shows that the predicted energy and angular distributions compare reasonably well with experiment, provided a strict Pauli blocking is used instead of the usual statistical implementation. Even better results are obtained by combining a strict Pauli blocking for the first collision with a statistical blocking for the subsequent collisions. An illustration is given by Fig. 8. The latter shows that the results of the INCL model are competing reasonably well with pre-equilibrium models, traditionally used in this energy range. One has however to keep in mind that composite production is neglected in this assessment. Experimentally, this

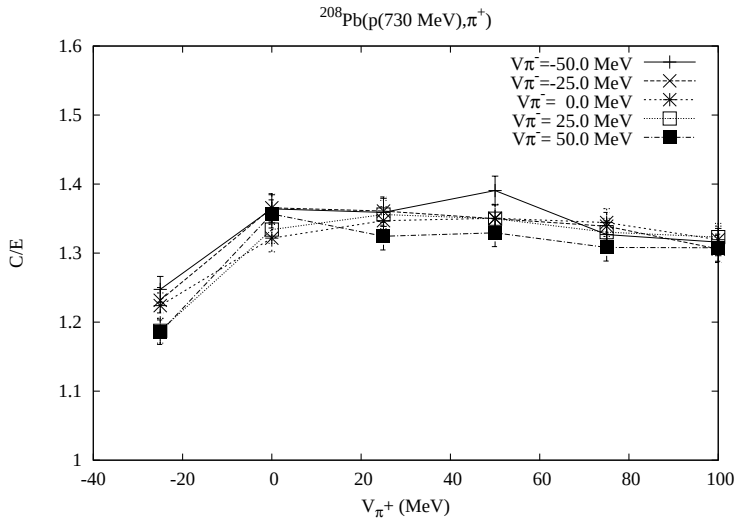

Figure 6: Ratio between calculated and experimental [21] total π^+ production cross section induced by 730 MeV proton on ^{208}Pb for various potential's depth.

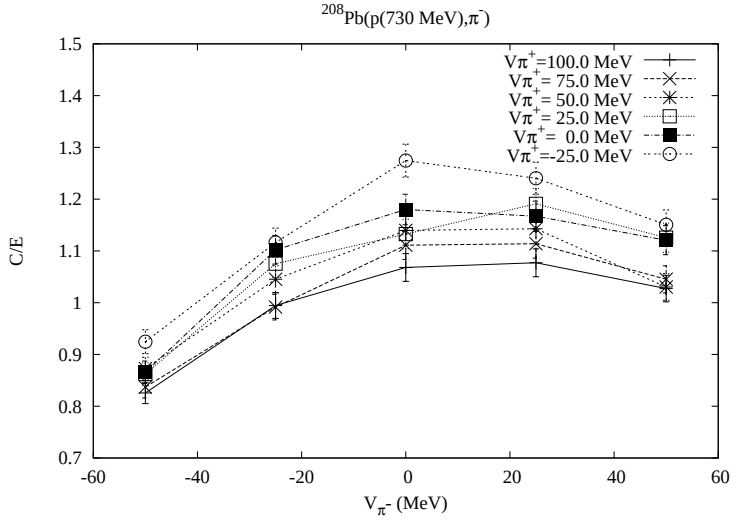

Figure 7: Same as fig. 6 for π^-.

process becomes comparatively more and more important as incident energy decreases.

3.3 Light composite emission

Based on surface coalescence model, we have implemented in INCL a relatively simple model which allows the production of light composites (d, t, ^3He and ^4He) in the cascade stage. When a nucleon fulfills the conditions to escape the nucleus, it is checked whether it can drag with him one or several neighboring nucleons in the phase space. A priority to the heaviest cluster is chosen. First we test if the largest composite can be built and escape. If not, smaller composites inside the original one are tested for emission, and so on. We refer to ref. [25] for more detail. Fig. 9 depicts the production of light composite produced with p(2.5 GeV) + Au. Here the evaporation code GEM is used instead of ABLA (which can not evaporate d t and ^3He). With these simple ingredients and without adjustements pertaining to the specific nature of the composites, the agreement with the experimental data of ref. [26] is satisfactory. As expected the implementation of light composite emission reduces the production of free neutrons and protons

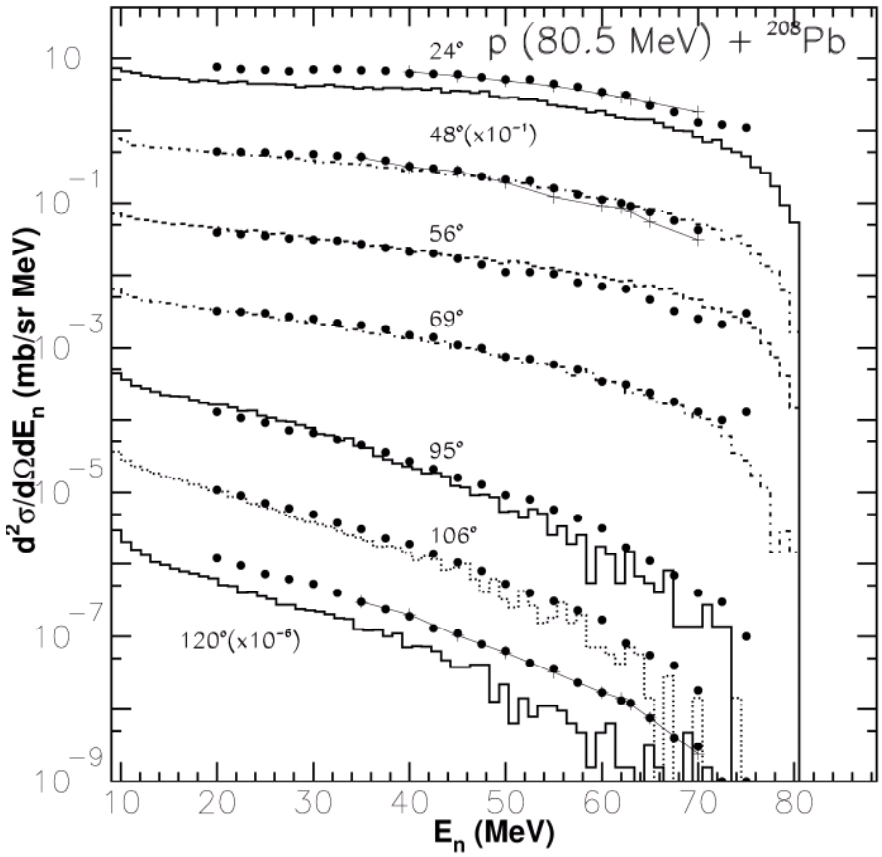

Figure 8: Double differential neutron cross section for p(80.5 MeV) + ^{208}Pb. Data (dots), taken from ref. [23], are compared with the results of the INCL model (histograms) and of the Multi-Step Direct (MSD) model of ref. [24]. Adapted from ref. [22].

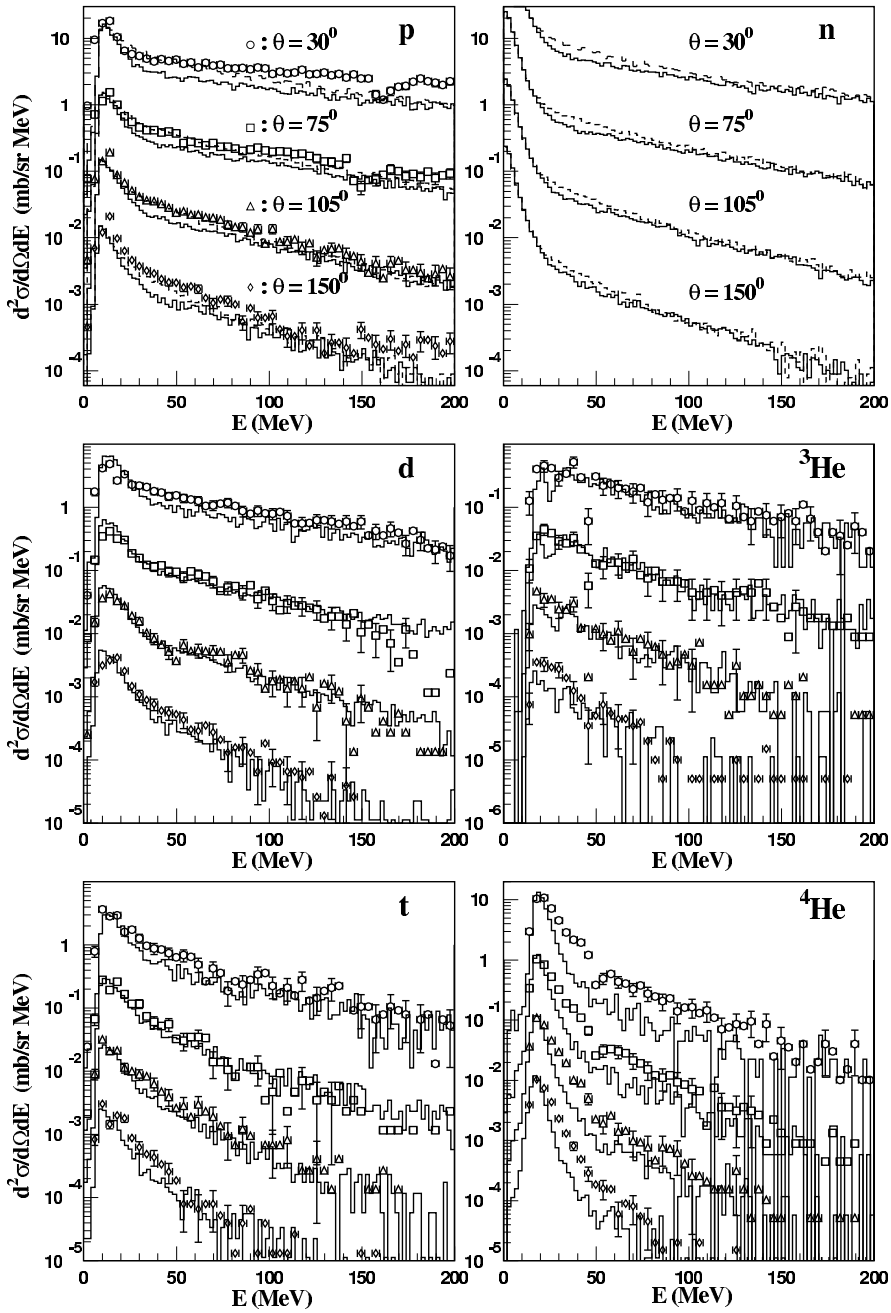

Figure 9: Comparison of the production spectra of light composite obtained with the INCL model supplemented by the composite emission model (histograms) with the experimental data in 2.5 GeV p + Au ref. [26]. Here the evaporation code of GEM is used.

during the cascade stage. But since other nucleons, which otherwise would have remained inside the nucleus, escape the nucleus, the total number of emitted neutrons is slightly increased.

4 CONCLUSION

The INCL4 code coupled to the evaporation-fission code ABLA reproduces quite well spallation observables induced by proton projectiles in the 200 MeV - 2 GeV range. Nevertheless specific observables, as the production of some spallation residues or the production of pions, present large discrepancies. This released version of the code can be used directly for thin or thick targets since it is implemented in the transport codes LAHET and MCNPX.

Keeping our philosophy of introducing as much as known physics as we can, we have introduced an isospin- and energy-dependent nuclear potential for nucleons, which is entirely borrowed from known phenomenology. The effect is rather small but improves the predictions. Despite a less precise phenomenology, we attempted also to introduce an isospin-dependent potential for pions. This implementation improves our results for pion production with reasonable values of the pion potential depth.

The INCL model was also tested with low incident energy (40-200 MeV) particles where the semi-classical approach is expected to fail. Using appropriate Pauli blocking, we obtained a reasonable prediction of double differential cross sections.

Finally we have included the production of light composites formed on the nuclear surface. It predicts surprisingly well the ratio and the order of magnitude of the yields of various species of composites on the scarce existing data.

All these modifications will be included in the forthcoming version of the INCL code.

5 REFERENCES

1. W. Haeck, G. Van den Eynde, Th. Aoust, H. Aït Abderrahim and P. D'hondt, *Proceedings of the International Workshop on P& T and ADS Development 2003*, Mol, Belgium 6-8 October 2003. http://www.sckcen.be/sckcen_en/activities/conf/conferences/20031006/contact.shtml 2003.
2. W. Botermans and R. Malfliet, *Phys. lett. B*, **215**, pp. 617 (1988).
3. V. E. Bunakov and G. V. Matvejev, *Z. Phys. A*, **322**, pp. 511 (1985).
4. J. Cugnon, *Nucl. Phys. A*, **387**, pp. 191 (1982).
5. J.J. Gaimard and K.H. Schmidt, *Nucl. Phys. A*, **531**, pp. 709 (1991). A.R. Junghans et al., *Nucl. Phys. A*, **629**, pp. 635 (1998).
6. *MCNPX2.4.0, Monte Carlo N-Particle Transport Code System for Multiparticle and High Energy Applications*,CCC-715, Sep. 2002.
7. A. Boudard, J. Cugnon, S. Leray and C. Volant, *Phys. Rev. C*, **66**, pp. 044615 (2002).
8. A. Boudard, J. Cugnon, J.-C. David, L. Donadille, S. Leray and C. Volant, *Proceedings of AccApp03*, San Diego, June 2003.

9. R.E. Chrien et al., *Phys. Rev. C*, **21**, pp. 1014 (1980). J.A. McGill et al., *Phys. Rev. C*, **29**, pp. 2004 (1984).
10. K.R. Cordell, *Nucl. Phys. A*, **352**, pp. 485 (1981).
11. G. Roy et al., *Phys. Rev. C*, **23**, pp. 1671 (1981).
12. J.Benlliure et al., *Nucl. Phys. A*, **683**, pp. 513 (2001). F. Rejmund et al., *Nucl. Phys. A*, **683**, pp. 540 (2001).
13. T. Enqvist et al., *Nucl. Phys. A*, **686**, pp. 481 (2001).
14. P. E. Hodgson, *The Nucleon Optical Potential*, World Scientific, (1994).
15. C. Mahaux and R. Sartor, *Adv. Nucl. Phys.*, **20**, pp. 1 (1991).
16. Th. Aoust and J. Cugnon, *Eur. Phys. J. A*, **21**, pp. 79 (2004).
17. S. Leray et al., *Phys. Rev. C*, **65**, pp. 044621 (2002).
18. J. Cugnon, Th. Aoust, P. Henrotte, A. Boudard, S. Leray and C. Volant, *Proceedings of ND2004, Int. Conf. on Nuclear Data for Science & Technology*, Santa Fe, Sep. 26 - Oct. 1, 2004.
19. M. M. Meier et al., *Radiation Eff.*, **96**, pp. 73 (1986).
20. M. B. Johnson and G. R. Satchler, *Ann. Phys.*, **248**, pp. 134 (1996).
21. D. R. F. Cochran et al., *Phys. Rev. D*, **6**, pp. 3085 (1972).
22. J. Cugnon and P. Henrotte, *Eur. Phys. J. A*, **16**, pp. 393 (2003).
23. M. Tranbandt et al., *Phys. Rev. C*, **39**, pp. 452 (1989).
24. R. Bonetti et al., *Phys. Rev. C*, **24**, pp. 71 (1981).
25. A. Boudard, J. Cugnon, S. Leray and C. Volant, *Nucl. Phys. A*, **740**, pp. 195 (2004).
26. A. Letourneau et al., *Nucl. Phys. A*, **712**, pp. 133 (2002).